Supplementary materials

Design strategy for effective supported Au-Pd catalysts for selective oxidation of 5-hydroxymethylfurfural under mild conditions

Tamara S. Kharlamova*[,1], Konstantin L. Timofeev[1], Denis P. Morilov[1], Mikhail A. Salaev[1], Andrey I. Stadnichenko[2], Olga A. Stonkus[2], Olga V. Vodyankina[1]

[1]Tomsk State University, Lenin Ave. 36, Tomsk, 634050, Russia
[2]Boreskov Institute of Catalysis, Lavrentiev Ave. 5, Novosibirsk, 630090, Russia
*kharlamova83@gmail.com, vodyankina_o@mail.com

1. Kinetic traces of HMF oxidation for the samples studied

The rate constant (k) for the HMF oxidation was determined from the kinetic traces (Figures S1-S4) using the first order rate law:

$$\frac{dC(HMF)}{dt} = -kC(HMF),$$

$$\ln\frac{C_o(HMF)}{C(HMF)} = kt \quad (1)$$

or

$$C(HMF) = C_o(HMF)e^{-kx} \quad (2)$$

Both data analysis using equation (1) and the curve fitting using the Exp2PMod1 model based on equation (2) were used.

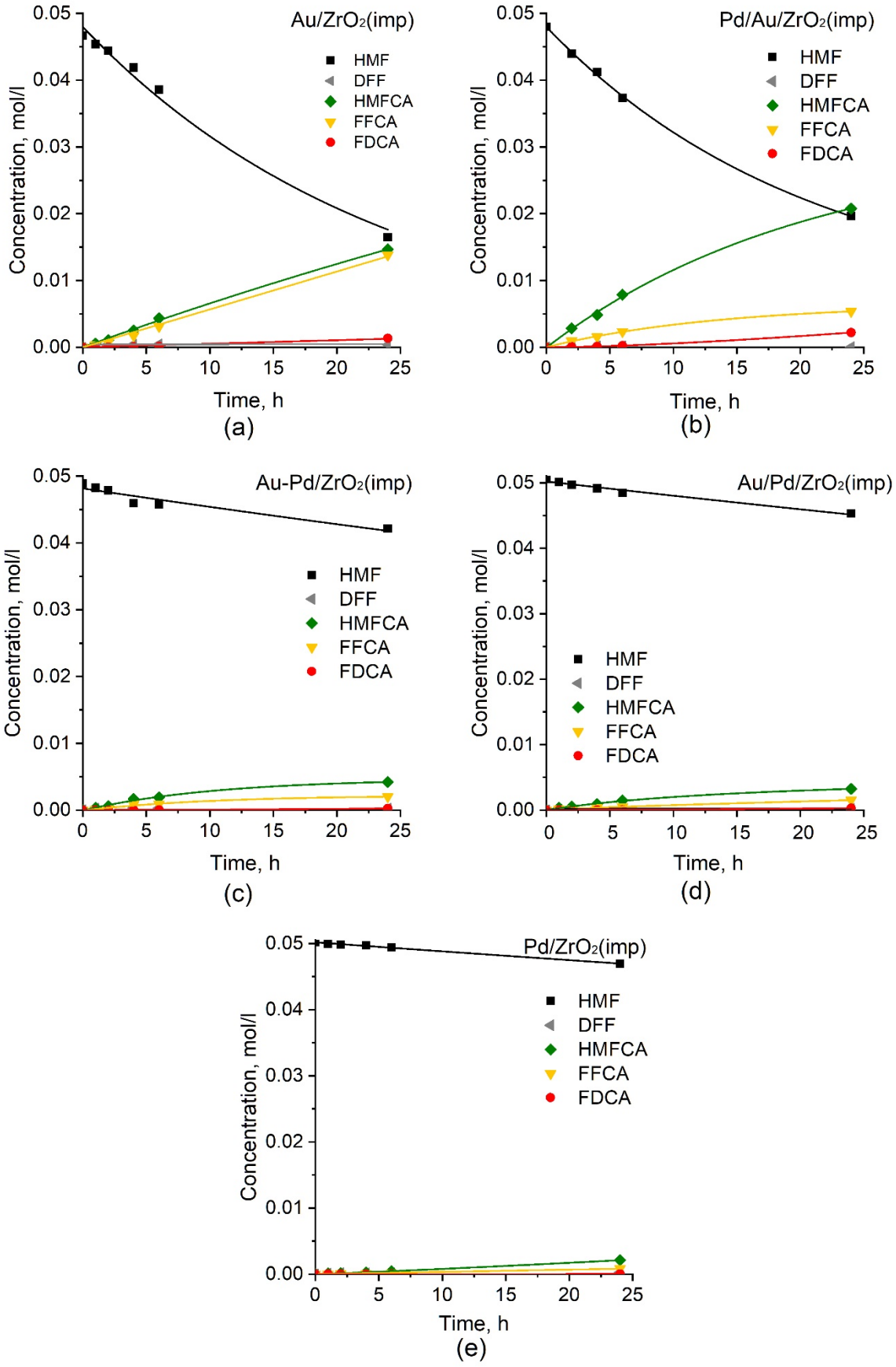

Figure S1. Kinetic traces of HMF oxidation for the imp series samples. Experimental conditions: HMF/metal/$NaHCO_3$ molar ratio of 1/0.01/4, 5 atm O_2, 80 °C.

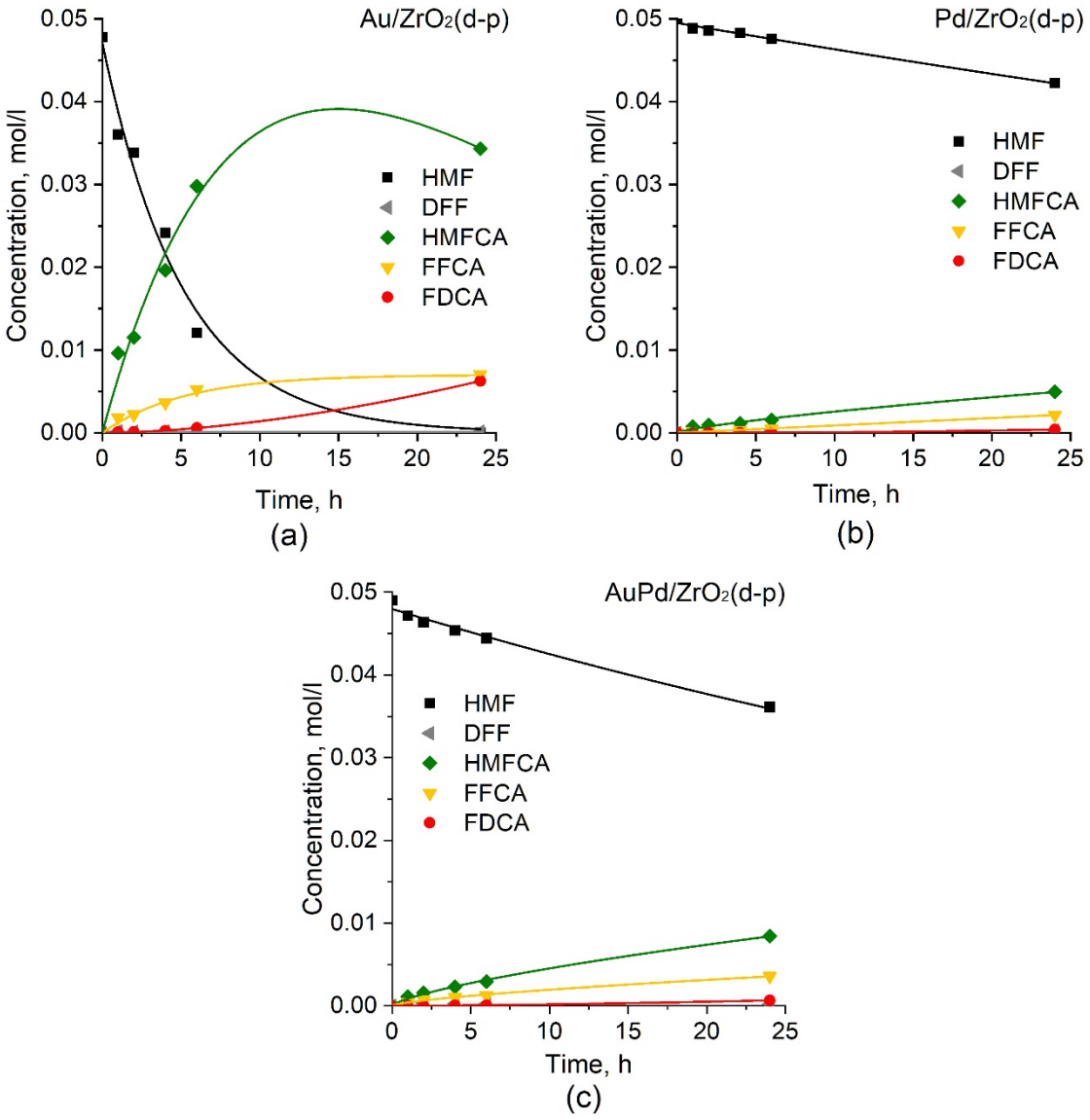

Figure S2. Kinetic traces of HMF oxidation for the d-p series samples. Experimental conditions: HMF/metal/$NaHCO_3$ molar ratio of 1/0.01/4, 5 atm O_2, 80 °C.

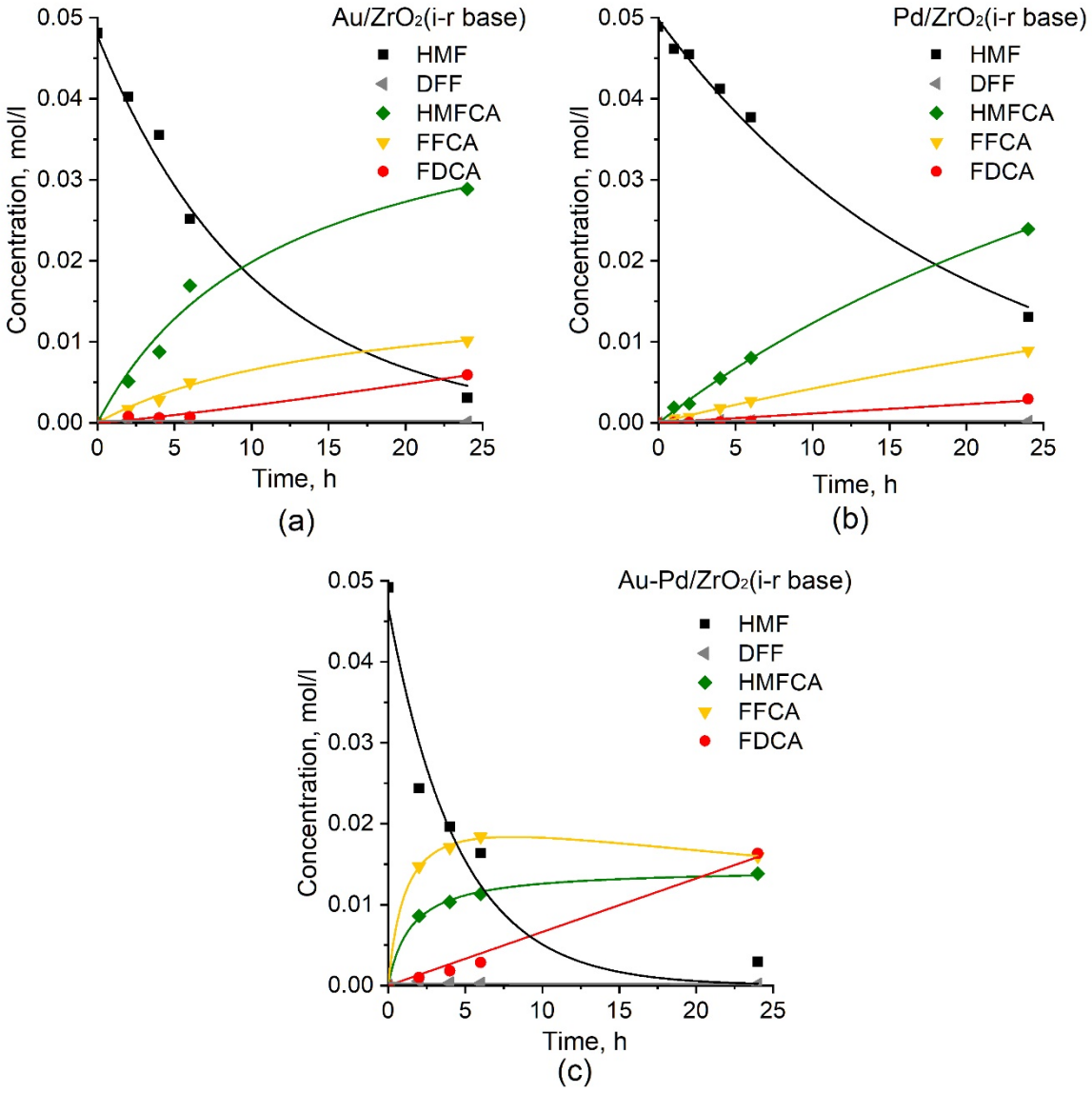

Figure S3. Kinetic traces of HMF oxidation for the i-r base series samples. Experimental conditions: HMF/metal/$NaHCO_3$ molar ratio of 1/0.01/4, 5 atm O_2, 80 °C.

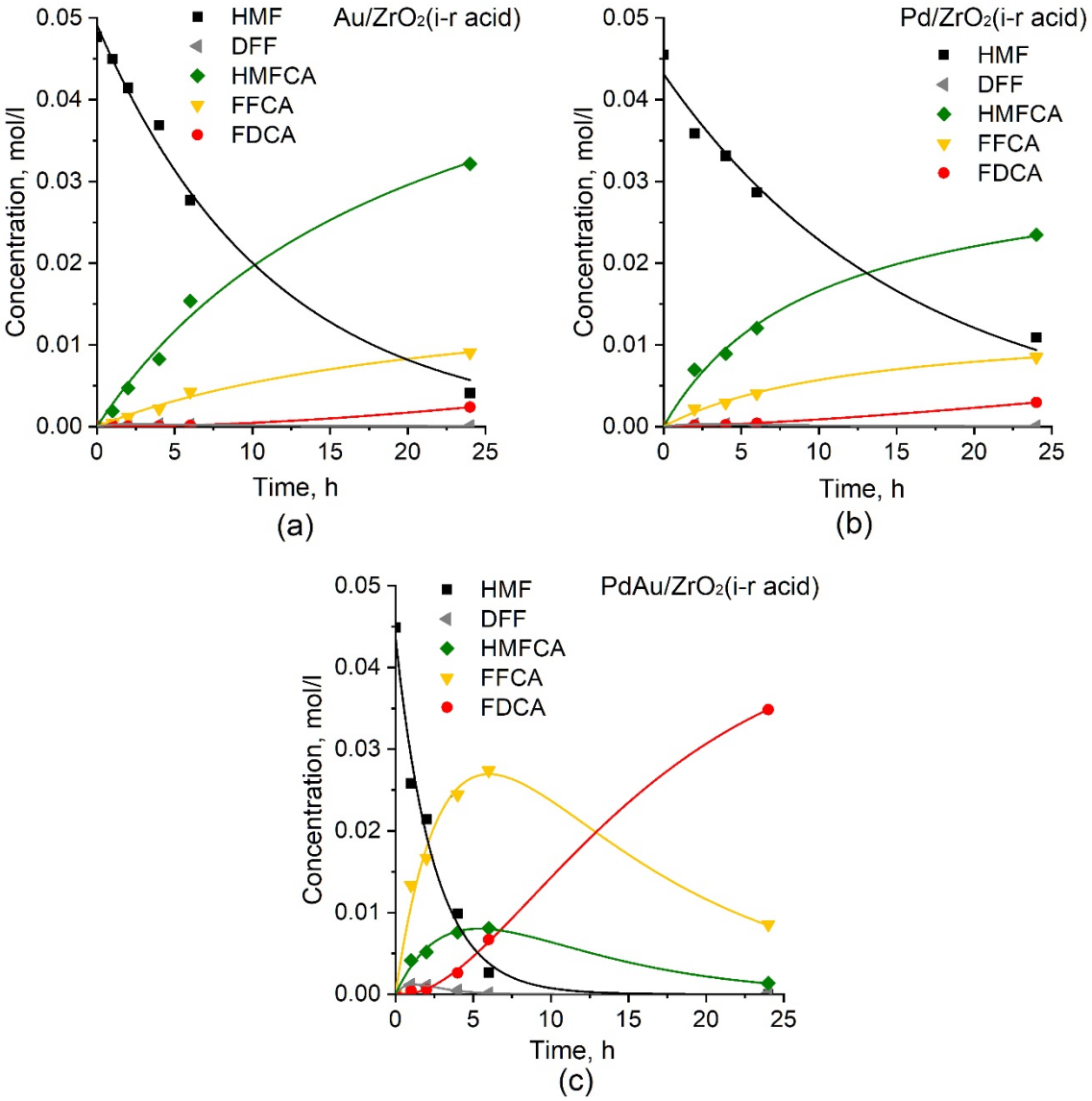

Figure S4. Kinetic traces of HMF oxidation for the i-r acid series samples. Experimental conditions: HMF/metal/$NaHCO_3$ molar ratio of 1/0.01/4, 5 atm O_2, 80°C.

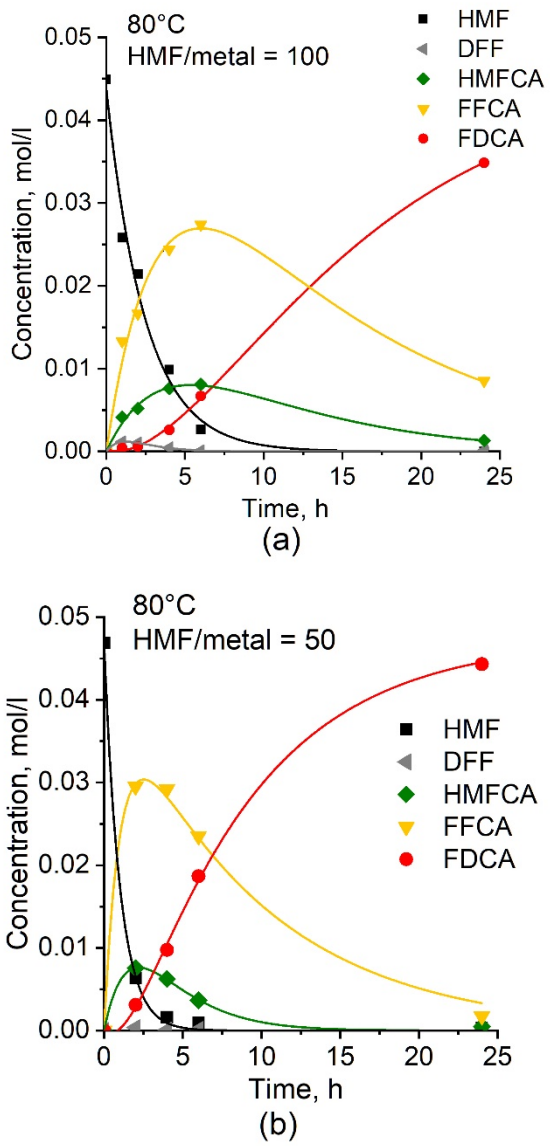

Figure S5. Kinetic traces of HMF oxidation for the Au-Pd/ZrO_2(i-r acid) sample for HMF/metal molar ratios of 100 (a) and 50 (b). Experimental conditions: HMF/$NaHCO_3$ molar ratio of 1/4, 5 atm O_2, 80°C (a).

2. Computational details and results

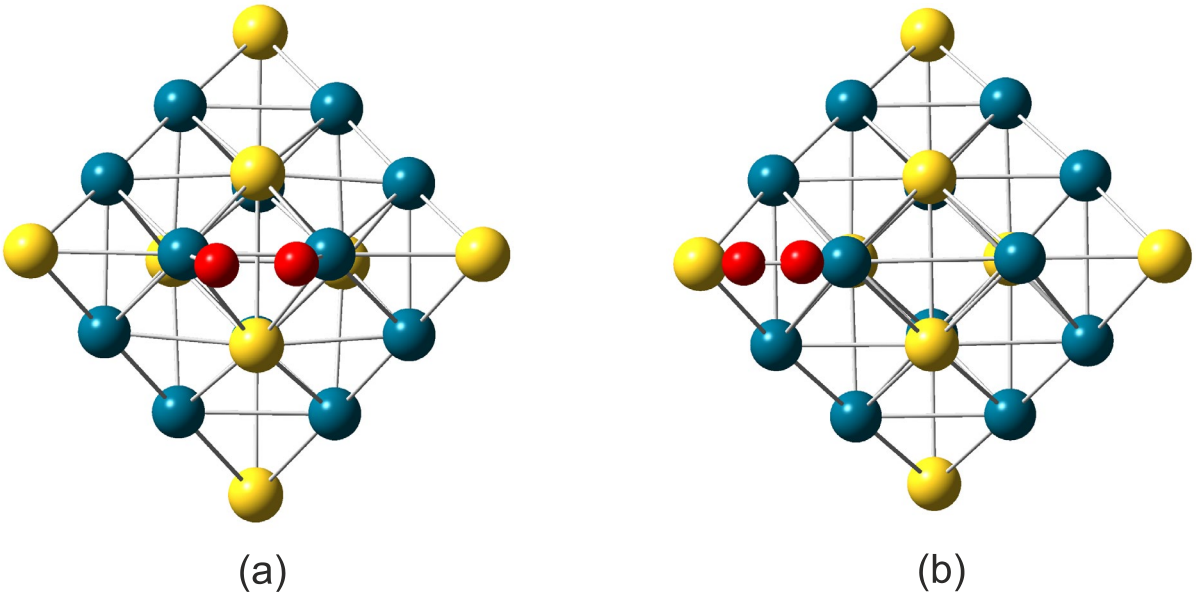

Figure S6. Models of O_2–cluster interaction for Au_8Pd_{12} clusters where substrate is located between: (a) two Pd atoms, (b) Pd and Au atoms. Color code: yellow, blue, and red balls correspond to gold, palladium, and oxygen atoms respectively.

Table S1. Binding energy (BE) and O-O distance (r(O-O))

Model	BE, kJ/mol	r(O-O), Å
O_2	-	1.257
$Au_{20}+O_2$	-166	1.521
$Pd_{20}+O_2$	-356	1.518
$Au_8Pd_{12}+O_2$ (Pd-Pd)	-335	1.478
$Au_8Pd_{12}+O_2$ (Pd-Au)	-225	1.491

3. X-ray diffraction data

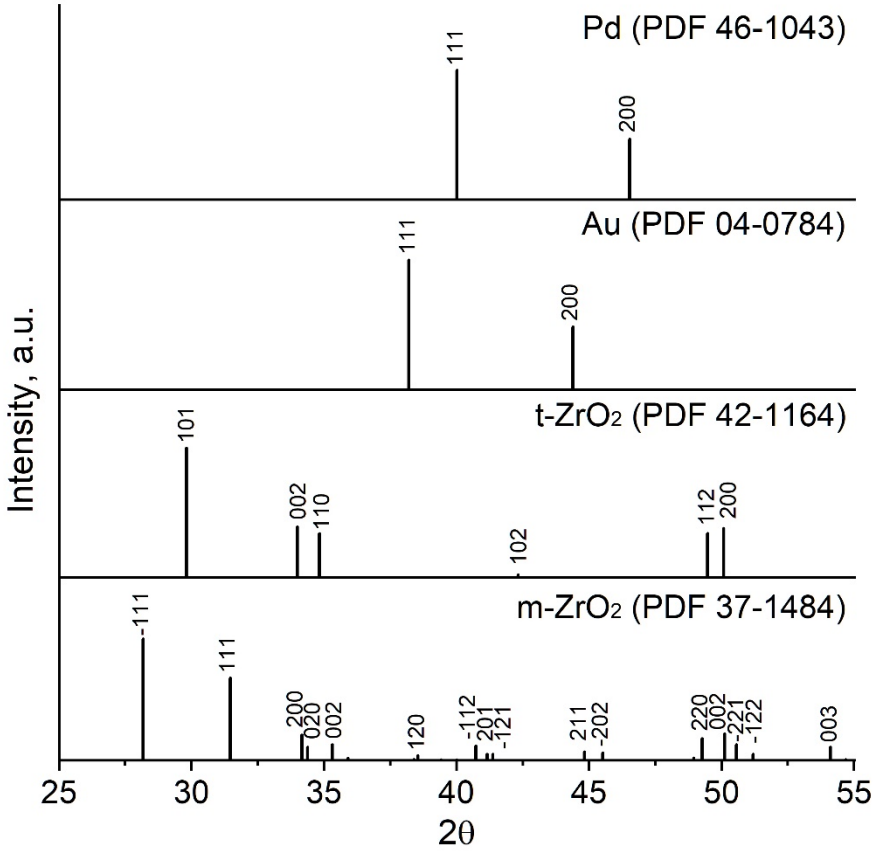

Figure S7. Stick patterns with the Miller indices according to ICDD PDF-4 used for ZrO_2, Pd, and Au phases.

4. Microscopy data

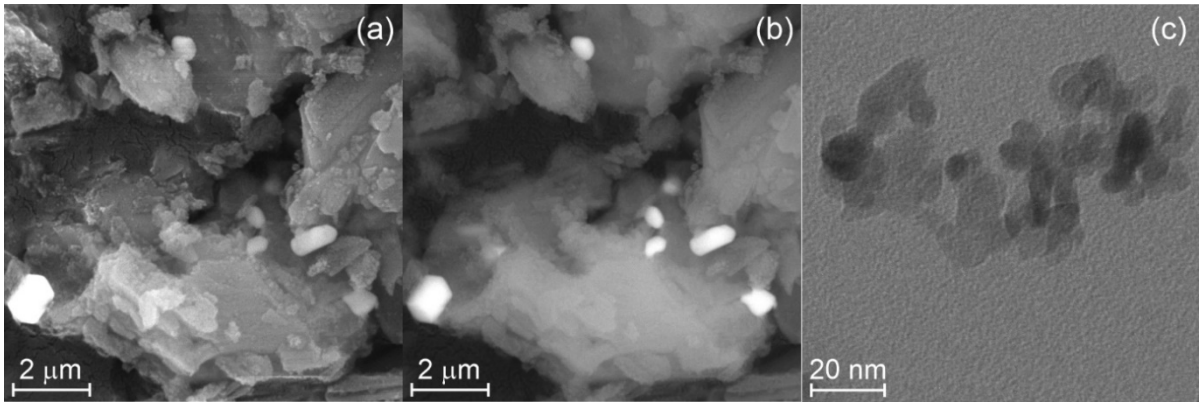

Figure S8. Typical SE-SEM (a), BSE-SEM (b), and TEM images for the Au/ZrO_2(imp) sample.

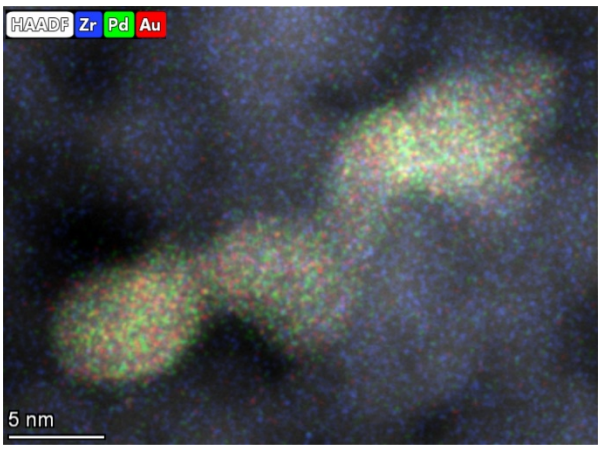

Figure S9. Typical HAADF-STEM with HR EDX mapping of single bimetallic NPs for the Au-Pd/ZrO2(i-r acid) sample.

Table S2. HR EDX mapping results for the Au-Pd/ZrO_2(i-r cit) sample.

Analyzed area	Fraction, at.%		Au/Pd
	Au	Pd	
Figure 5b	2.0±0.7	2.7±0.8	0.43/0.57
Figure 5c	1.9±0.3	2.6±0.4	0.42/0.58
Figure 5d	13.1±2.0	13.5±2.1	0.49/0.51
Image not shown	4.0±0.6	4.3±0.7	0.48/0.52
Image not shown	8.2±1.2	8.1±1.2	0.50/0.50

5. Electrokinetic and adsorption properties of the ZrO_2 support

The electrokinetic properties of the ZrO_2 water dispersion were studied by electrophoretic light scattering (ELS) using the phase analysis light scattering (PALS) technique on the Omni S/N analyzer (Brookhaven, NY, USA) equipped with the BI-ZTU autotitrator (Brookhaven, NY, USA). For the study, the samples were dispersed in a distilled water at a concentration of 25 mg/L using ultrasound for 10 min. To determine the pH of the isoelectric point (IEP), the dispersion was titrated using the diluted KOH solutions (0.001 and 0.1 mol/L).

The water dispersion of ZrO_2 was characterized by an initial pH of ~5 and a zeta potential of 33 ± 1 mV (Figure S10). The pH increase resulted in a rapid decrease in the surface charge, with the IEP being at a pH of 5.9.

Adsorption of metal precursors and citric acid on ZrO_2 was carried out under the following conditions: for metal precursors, 1 ml of a solution of H_2PdCl_4 or $HAuCl_4$ with a concentration ranging from 0.005 to 0.075 mol/l was added to 250 mg of ZrO_2; for citric acid, 25 ml of a citric acid solution with the same concentration range was added to 1 g of ZrO_2. The resulting suspensions were left for 3 h in a thermostated room at a temperature of 20°C. The suspensions were then centrifuged or filtered, and the resulting solution was analyzed.

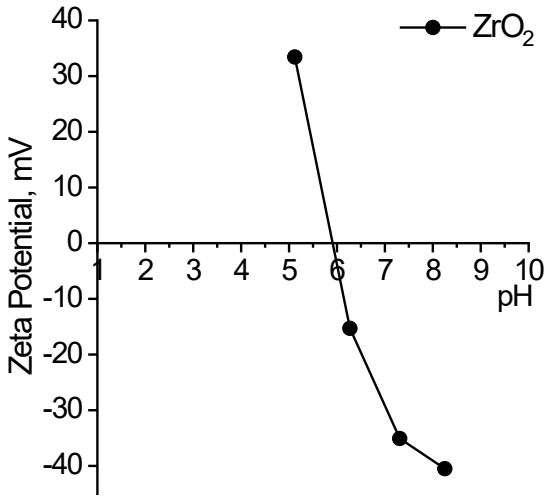

Figure S10. Dependence of zeta potential of ZrO_2 on pH of water suspension.

In the case of metal precursors, the solutions were analyzed spectrophotometrically on the SM 2203 spectrofluorimeter (SOLAR, Belarus) in the wavelength range from 220 to 600 nm. The concentrations of the substances were determined using the calibration dependence obtained for the solutions with a given concentration. In the case of citric acid, the amount of adsorbed substance was determined by the potentiometric titration [1]. The filtrate was titrated potentiometrically with an aqueous KOH solution (0.1 mol/L) using the pH meter/ionometer ITAN (LLC SPE Tomanalit, Tomsk, Russia) to measure the titration potential.

The amount of adsorbed substance was determined according to the formula:

$$a = \frac{(C_0 - C_e) \times V_o}{m},$$

where a is the amount of adsorbed substance, mol/g; C_0 is an initial concentration of a solution, mol/l; C_e is an equilibrium concentration of a solution, mol/l; m is a support mass, g; V_o is a volume of solution, l.

The adsorption of $H_2[PdCl_4]$, $H[AuCl_4]$, and citric acid on the ZrO_2 support is described by the Langmuir adsorption isotherm equation:

$$a = \frac{a_m \cdot K_L \cdot C_e}{1 + K_L \cdot C_e},$$

where a is the adsorbate sorption capacity, mmol/g; a_m is the maximal adsorption capacity, mmol/g; K_L is the Langmuir constant, l/mol; C_e is an equilibrium concentration of the Pd or Au precursors, mol/l. Table S2 shows the adsorption isotherm parameters. Considering the IEP of ZrO_2 (Figure S9), the adsorption of acids on the support is linked to the one of the corresponding anions.

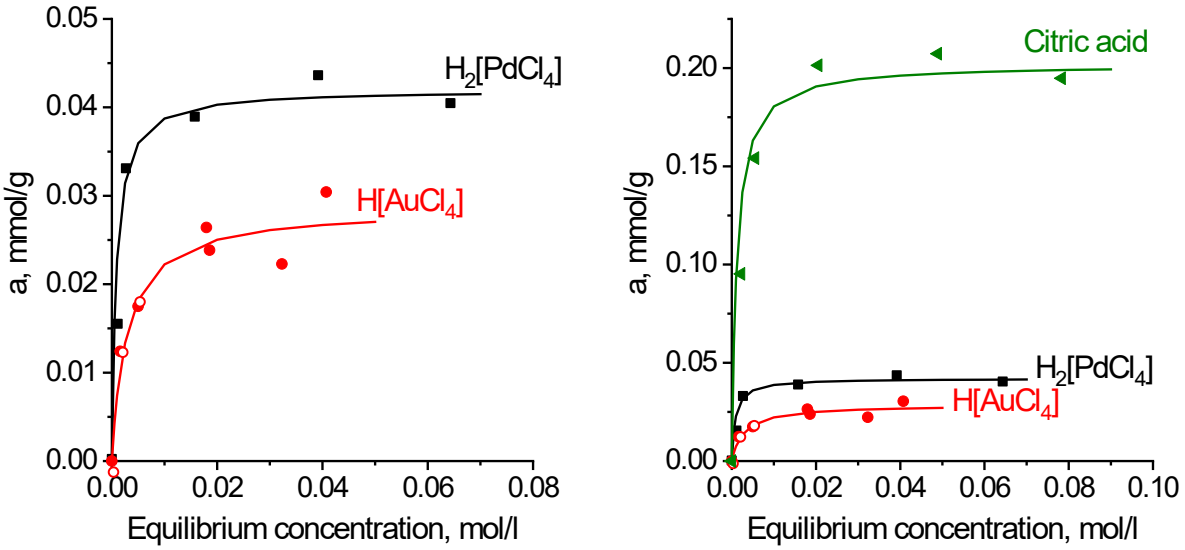

Figure S11. Adsorption isotherms of $H_2[PdCl_4]$, $H[AuCl_4]$, and citric acid on ZrO_2 support from aqueous solutions of Pd and Au precursors at 19 °C. Scatter are experimental data, lines are model.

Table S2. Characteristics of adsorption of $H_2[PdCl_4]$ and $H[AuCl_4]$ on the ZrO_2 support from aqueous solutions of Pd and Au precursors at 19 °C.

Adsorbate	K_L, l/mol	a_m, mmol/g
$H_2[PdCl_4]$	1190	0.042
$H[AuCl_4]$	350	0.029
citric acid	839	0.202

6. X-ray photoelectron spectroscopy data

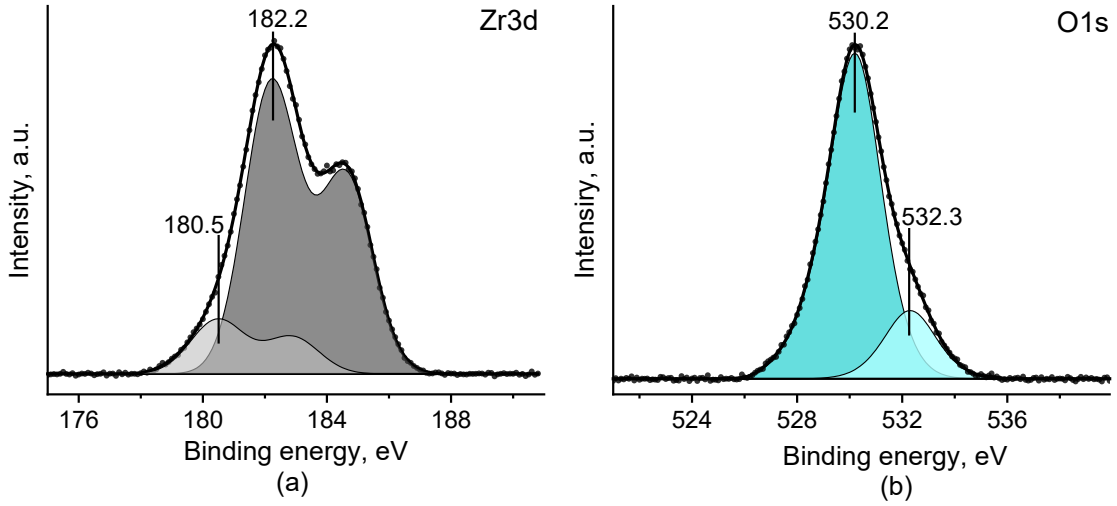

Figure S12. Typical Zr3d and O1s spectra exemplified by those for the Au/ZrO_2(i-r cit) sample.

7. Performance and reusability of Au-Pd/ZrO_2(i-r acid) catalyst

Reducing the HMF/metal molar ratio to 50 or increasing the temperature to up to 100 °C when using $NaHCO_3$ as an alkaline agent (pH is ~8) leads to a significant increase in the observed activity of the Au-Pd/ZrO_2(i-r acid) sample (Figure S12, Table S3). Almost complete HMF conversion and ~40% FDCA yield are observed at 80°C already in 6 h, and in 24 h, the FDCA yield is ~97%. Increasing the temperature to up to 100°C at the HMF/metal molar ratio = 100 make it possible to increase the FDCA yield for the Au-Pd/ZrO_2(i-r acid) sample to 57% in 6 h of reaction (Table S3) and to 65% in 7 h of reaction, and almost complete HMF conversion is observed in 2 h.

Table S3. Catalytic properties of the Au-Pd/ZrO_2(i-r acid) sample under different conditions.

Base / pH	T, °C	HMF/ metal	X(HMF), %	Product yield, %				CB***, %
				HMFCA	FFCA	FDCA	DFF	
$NaHCO_3$ / 8	80	100	94.1	18.0	61.0	14.9	0.2	96.3
$NaHCO_3$ / 8	80	50	98.0	7.8	50.1	39.8	0.3	99.2
$NaHCO_3$ / 8**	80	50	100	-	2.3	97.7	-	99.2
$NaHCO_3$ / 8	100	100	100	0.6	42.4	57.0	-	>99
NaOH / 12	80	100	100	19.1	6.1	33.0	0.3	66

*Results in 5 h of the rection. **Results in 24 h of the rection. ***CB is carbon balance

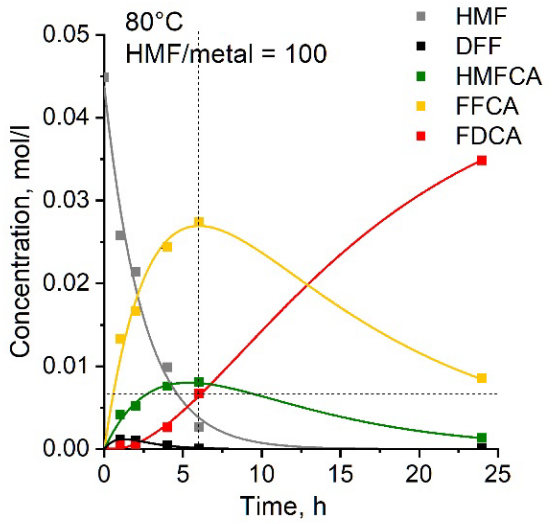

(a)

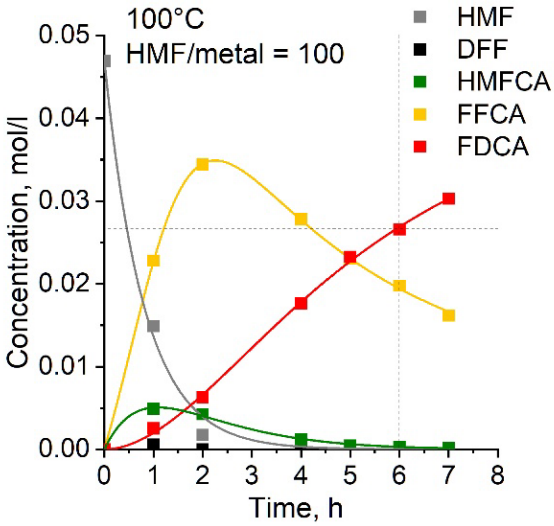

(b)

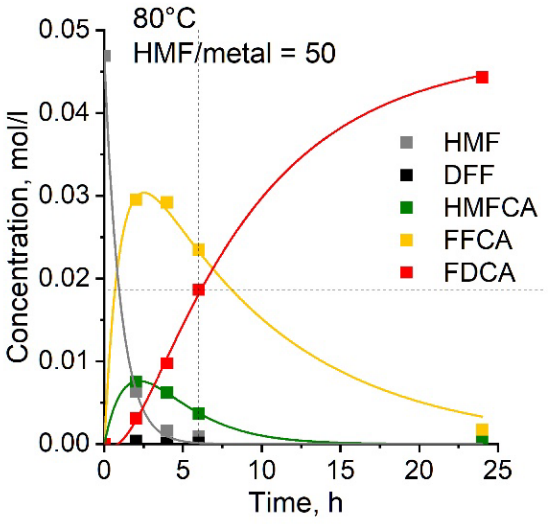

(c)

Figure S13. Kinetic traces of HMF oxidation for the Au-Pd/ZrO_2(i-r acid) sample under 5 atm O_2, HMF/$NaHCO_3$ molar ratio of 1/4, and different temperature and/or HMF/metal molar ratio: 80 °C, HMF/metal = 100 (a); 100 °C, HMF/metal = 100 (b); 80 °C, HMF/metal = 50 (c).

The Au-Pd/ZrO_2(i-r acid) catalyst showed high stability in two subsequent cycles for 5 h at 90 °C (Figure 6). In these recycles, the complete HMF conversion was observed, with the FFCA being the main product (selectivity >70%) and the FDCA yield being 11%. In the subsequent two cycles, a gradual decrease in the HMF conversion was observed, but it did not decline lower than 69% in the fourth recycle. This was accompanied by a decrease in the FFCA and FDCA selectivities and an increase in the HMFCA and DFF selectivities primarily due to the decrease of the HMF conversion level. No leaching was confirmed for the Au-Pd/ZrO_2(i-r acid) catalyst, and the observed decrease in its activity was assigned to particle size increase (the crystallite size for alloy increased up to 12 nm after recycling, Table S4) primarily due to the sintering and/or recrystallization of NPs in agglomerates.

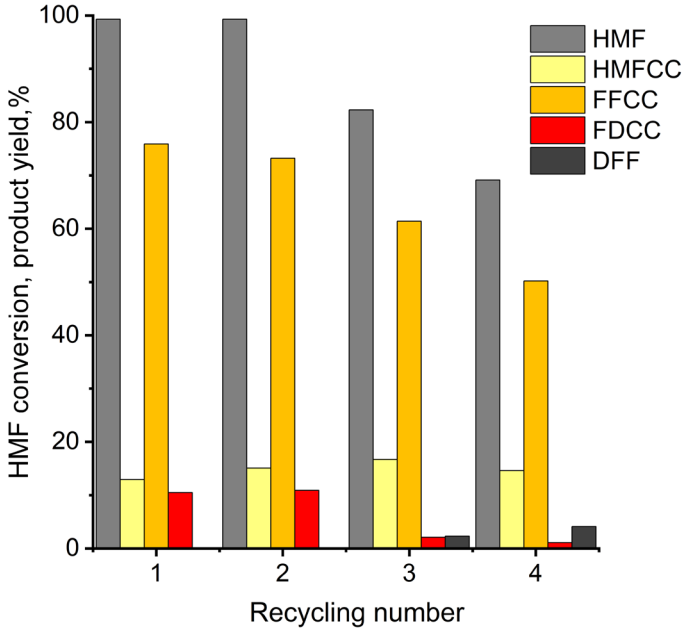

Figure S14. Stability of the Au-Pd/ZrO_2(i-r acid) catalyst during the recycling uses for the aerobic HMF oxidation. Experimental conditions: HMF/metal/$NaHCO_3$ molar ratios of 1/0.01/4, 5 atm O_2, 90 °C, 5 h.

Table S4. Characteristics of the Au-Pd/ZrO_2(i-r acid) sample before and after reusability test.

Sample	Content, wt.%		XRD data	
	Au	Pd	D_{XRD}, nm	*a*, Å
Initial	1.4	0.7	7	3.997
After reusability test	1.4	0.7	12	3.998

These results indicate a rather good stability of the Au-Pd/ZrO_2(i-r acid) catalyst, which is notably greater than those of Au-Pd/MgO and Au-Pd/HT catalysts rapidly losing their activity due

to the support dissolution into the reaction solution [2]. However, the improvement of the alloy dispersion in the AuPd/ZrO_2 catalysts by controlling the rate of reduction of Pd and Au precursors from the solution with $NaBH_4$ is required.

References

1 Timofeev K.L., Kulinich S.A., Kharlamova T.S. NH_2-Modified UiO-66: Structural Characteristics and Functional Properties, *Molecules* 2023, 28(9), 3916. https://doi.org/10.3390/molecules28093916

2. Wan X., Zhou C., Chen J., Deng W., Zhang Q., Yang Y., Wang Y. Base-Free Aerobic Oxidation of 5-Hydroxymethyl-furfural to 2,5-Furandicarboxylic Acid in Water Catalyzed by Functionalized Carbon Nanotube-Supported Au–Pd Alloy Nanoparticles, ACS Catal. 2014, 4, 7, 2175–2185. https://doi.org/10.1021/cs5003096